5 Supplementary Material

5.1 Additional Parameters Description for the New PSA Model

Param	Description	Range	Unit
μ	max proliferation rate	0.001 – 0.09	day^{-1}
μ_1	max proliferation rate (AD cells)	0.001 – 0.09	day^{-1}
μ_2	max proliferation rate (AI cells)	0.001 – 0.09	day^{-1}
q_1	min AD cell quota	0.41 – 1.73**	$\text{nmol}\cdot\text{day}^{-1}$
q_2	min AI cell quota	0.01 – 0.41**	$\text{nmol}\cdot\text{day}^{-1}$
b	baseline PSA production rate	0.0001 – 0.1	$\mu\text{g}\cdot\ \text{nmol}^{-1}\cdot\text{day}^{-1}$
σ	tumor PSA production rate	0.001 – 1	$\mu g\cdot\text{nmol}^{-1}\cdot\text{L}^{-1}\cdot\text{day}^{-1}$
ε	PSA clearance rate	0.0001 – 0.1	day^{-1}
d_1	max AD cell death rate	0.001 – 0.09	day^{-1}
d_2	max AI cell death rate	0.01 – 0.001	day^{-1}
δ_1	density death rate	1 – 90	$\text{L}^{-1}\cdot\text{day}^{-1}$
δ_2	density death rate	1 – 90	$\text{L}^{-1}\cdot\text{day}^{-1}$
R_1	AD death rate half-saturation	0 – 3	$\text{nmol}\cdot\text{L}^{-1}$
R_2	AI death rate half-saturation	1 – 6	$\text{nmol}\cdot\text{L}^{-1}$
c	maximum mutation rate	0.00001 – 0.0001	day^{-1}
K	mutation rate half-saturation level	0.8 – 1.7	$\text{nmol}\cdot\text{day}^{-1}$
m	diffusion rate from A to Q	0.01 – 0.9	day^{-1}
$x_1(0)$	Initial subpopulation of AD cells	0.009 – 0.02	L
$x_2(0)$	Initial subpopulation of AI cells	0.0001 – 0.001	L

Table 5: Additional parameter definition and range provided in [21]. ** Minimum AD and AI cell quota should be patient specific, therefore we choose the ranges for q_1 and q_2, respectively, to be $(b + 0.2, b + 0.5)$ and $(0.01, b + 0.2)$, where b is the minimum androgen value data for each individual patient.

5.2 Synergistic Effects Between Drug Therapies

To build on the Dosage Variation Simulations we consider simulations broader range of dosage levels and over two time intervals: during the first on-drug period (0.5 cycle) of

therapy and after 1.5 cycles of therapy (corresponding to the parameter-fitting interval used for all patients).

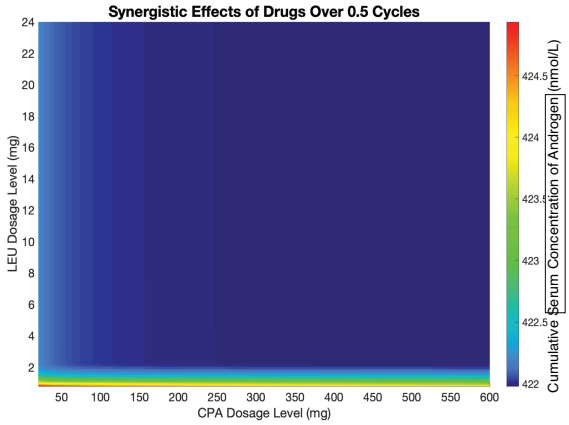

(a) 0.5 cycles > 10% Normal Drug Doses

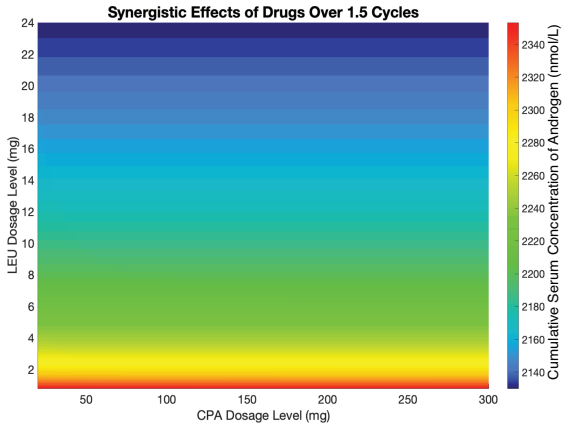

(b) 1.5 cycles > 10% Normal Drug Doses

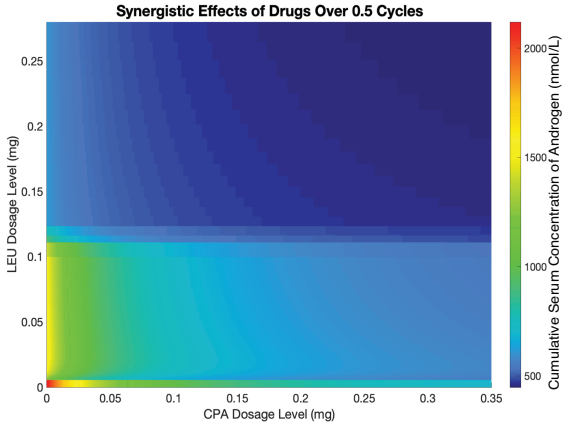

(c) 0.5 cycles Small Drug Doses

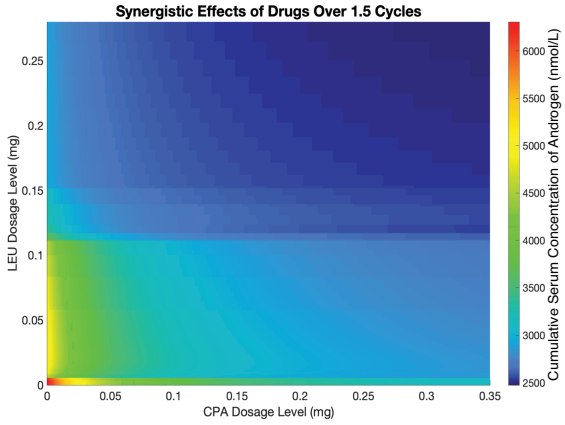

(d) 1.5 cycles Small Drug Doses

Figure 10: Simulated total androgen production across different time scales and dosage ranges from the New Androgen Model using parameters and dosing times for Patient 15. (The color scales differ in each panel.) (a) Heat map showing cumulative serum concentration of androgen over 0.5 cycle of therapy for LEU dosage levels from 0.8–24 mg and CPA dosages from 20–60 mg (a 550×550 grid is shown). (b) Cumulative serum concentration of androgen over 1.5 cycles of therapy using the same dosage ranges as (a). (c) Cumulative serum concentration of androgen over 0.5 cycles of therapy for LEU dosages from 0–0.14 mg and CPA dosages from 0–0.25 mg. (d) Cumulative serum concentration of androgen 1.5 cycles of therapy for LEU dosages from 0–0.16 mg and CPA dosages from 0–2 mg.

Figure 10 shows the results of simulations of the New Androgen Model using the dosage administration times for Patient 15 and the parameters in Table 2. Dosages of CPA and LEU are simulated at various ranges of dosages: close to the usual clinial ranges in panels (a) and (b), and at small dosages in (c) and (d), forming a 550×550 grid. For each choice of drug dosage, the New Androgen Model is run for either 0.5 cycles of treatment (panels (a) and (c)) or for 1.5 cycles (panels (b) and (d)). In all cases, the net production of androgen, i.e., the integral of $A(t)$ as simulated by Eq. (8) is estimated over the corresponding interval.

Over the first half-cycle of treatment (corresponding to the first on-drug period), the cumulative serum concentration of androgen predicted by the model is largely insensitive to dosage over the simulated ranges, as shown in Fig. 10(a). In contrast, the cumulative serum concentration of androgen production over 1.5 cycles of therapy, which includes the first treatment hiatus, decreases approximately linearly with LEU dosage. Because the modeled drug effects are multiplicative, androgen production is suppressed whenever the level of either CPA or LEU is sufficiently high (cf. Fig. 3). Furthermore, as described above, androgen production becomes insensitive to CPA dosage after LEU desensitizes the gonadotropic pathway, which occurs 7 to 21 days after initial injection [36]. LEU also has slower clearance rates than CPA (cf. Table 1) and so is effective longer.

Both Figures 10a and 10c are over 281 days, which represents the first 0.5 cycles for patient 15. In contrast to Figure 10a, Figure 10c focuses on the dynamics around very small doses for both drugs. The most interesting dynamics happen for LEU dosage of 0.0055mg. The sharp increase of androgen at this value occurs due to a L^* value of 0.0055mg for patient 15. If the LEU dosage remains below the L^* level, the LEU effect, Equation (15), never proceeds to the spike and desensitizing behavior. The lack of spiking and desensitizing behavior in androgen production aligns with the pharmacology report on LEU [38]. The second sharp increase in cumulative serum concentration of androgen occurs around a dosage of 0.11mg for LEU. In this case, the increase is due to the feature that doses between 0.0055mg-0.11mg lead to a spiking and desensitizing phase, but do not maintain levels above L^* long enough for desensitization to occur, only spiking. However, above the 0.11mg dosage level, desensitization occurs and a drop in androgen occurs more predictably as seen in 10a. Given the amount of time between dosages of the drugs, as seen in Figure 3 from the main paper, it should be noted that the clinical administration of either drug at such low levels is not consistent with treatment of prostate cancer.

5.3 New PSA Model Sensitivity Analysis

5.3.1 Local Sensitivity Analysis

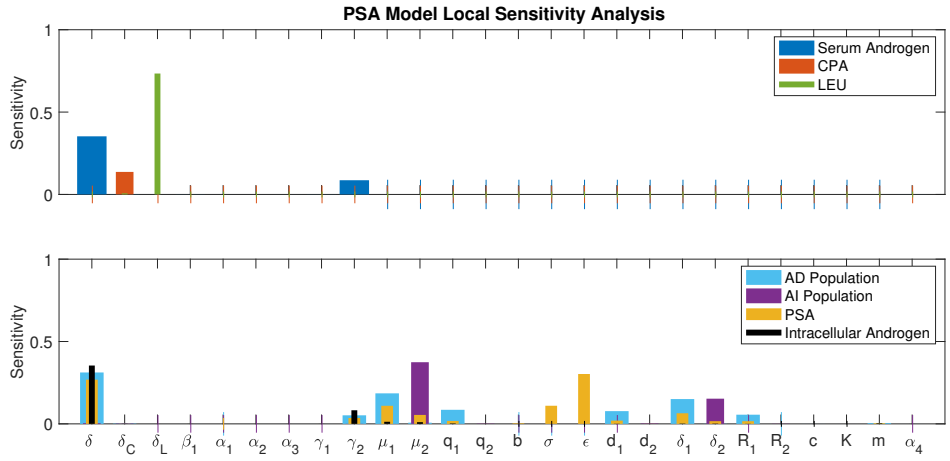

Figure 11: **(Top)** Normalized sensitivity for serum androgen (strong blue), LEU mass (vivid orange), and CPA mass (dark green) with respect to each parameter of the full model. **(Bottom)** Normalized sensitivity for androgen-dependent population (soft blue), androgen-independent population (dark moderate magenta), intracellular androgen (vivid yellow) and prostate-specific antigen (black) with respected to each parameter of the full New PSA Model. **Note**: δ, δ_1, δ_2, β_1, α_1, α_2, α_3, α_4, γ_1 and γ_2 parameter values are those of the New Androgen Model depicted in Figure 8.

5.3.2 Global Sensitivity Analysis

In this section, we use Sobol's indices [64], a variance-based method, to perform global sensitivity analysis (GSA). Consider a nonlinear mathematical model, f, with scalar output, y:

$$y = f(q) \tag{27}$$

where $q = \left[q_1, q_2, \ldots, q_p\right] \in Q_p \subseteq \mathbb{R}^p$ with q is a vector of model parameters and Q_p is the admissible sample space for model parameters.

The first-order Sobol's indices are defined by:

$$S_i = \frac{\text{var}\left[\mathbb{E}(y|q_i)\right]}{\text{var}(y)} \tag{28}$$

with S_i is the influential measurement of parameter q_i on the variance of model output y. The total-effect Sobol's indices that account for both first-order and higher-order effects are given by:

$$S_{Ti} = 1 - \frac{\text{var}\left[\mathbb{E}(y|q_{\sim i}\right]}{\text{var}(y)} = \frac{\mathbb{E}\left[\text{var}(y|q_{\sim i})\right]}{\text{var}(y)}. \tag{29}$$

However, it is computationally expensive to use the original Sobol's indices method. Instead, we used a numerical approximation approach that was introduced and improved in [65, 66, 67]. The algorithm is later summarized in [68] and described as follows:

1. Create two $M \times p$ matrices, $\boldsymbol{A}$ and $\boldsymbol{B}$:

$$\boldsymbol{A} = \begin{bmatrix} q_1^1 & \dots & q_i^1 & \dots & q_p^1 \\ \vdots & & & & \vdots \\ q_1^M & \dots & q_i^M & \dots & q_p^M \end{bmatrix}, \quad \boldsymbol{B} = \begin{bmatrix} \hat{q}_1^1 & \dots & \hat{q}_i^1 & \dots & \hat{q}_p^1 \\ \vdots & & & & \vdots \\ \hat{q}_1^M & \dots & \hat{q}_i^M & \dots & \hat{q}_p^M \end{bmatrix}$$

   with each entries q_i^j and $\hat{q}_i^j$ are quasi-random numbers being drawn uniformly from the range of the ith parameter at the jth realization. Here, we chose $M = 1000$, i.e. 1000 realizations.

2. Create p matrices $\boldsymbol{C}_{\boldsymbol{A}}^i$:

$$\boldsymbol{C}_{\boldsymbol{A}}^i = \begin{bmatrix} q_1^1 & \dots & \hat{q}_i^1 & \dots & q_p^1 \\ \vdots & & & & \vdots \\ q_1^M & \dots & \hat{q}_i^M & \dots & q_p^M \end{bmatrix}$$

   by replacing the ith column of matrix $\boldsymbol{A}$ by the ith column of matrix $\boldsymbol{B}$. And create p matrices $\boldsymbol{C}_{\boldsymbol{B}}^i$:

$$\boldsymbol{C}_{\boldsymbol{B}}^i = \begin{bmatrix} \hat{q}_1^1 & \dots & q_i^1 & \dots & \hat{q}_p^1 \\ \vdots & & & & \vdots \\ \hat{q}_1^M & \dots & q_i^M & \dots & \hat{q}_p^M \end{bmatrix}$$

   by replacing the ith column of matrix $\boldsymbol{B}$ by the ith column of matrix $\boldsymbol{A}$.

3. Compute $M \times 1$ vectors of the model outputs:

$$y_{\boldsymbol{A}} = f(\boldsymbol{A}), \quad y_{\boldsymbol{B}} = f(\boldsymbol{B}), \quad y_{\boldsymbol{C}_{\boldsymbol{A}}^i} = f(\boldsymbol{C}_{\boldsymbol{A}}^i), \quad y_{\boldsymbol{C}_{\boldsymbol{B}}^i} = f(\boldsymbol{C}_{\boldsymbol{B}}^i)$$

   with $y_{\boldsymbol{A}}^j$, $y_{\boldsymbol{B}}^j$, $y_{\boldsymbol{C}_{\boldsymbol{A}}^i}^j$, and $y_{\boldsymbol{C}_{\boldsymbol{B}}^i}^j$ correspond to the model output evaluated at the jth row vectors of parameters of matrices $\boldsymbol{A}$, $\boldsymbol{B}$, $\boldsymbol{C}_{\boldsymbol{A}}^i$, and $\boldsymbol{C}_{\boldsymbol{B}}^i$, respectively.

4. Append $y_{\boldsymbol{A}}$ and $y_{\boldsymbol{B}}$ to obtain $2M \times 1$ vector $y_{\boldsymbol{D}}$.

$$y_{\boldsymbol{D}} = \begin{bmatrix} y_{\boldsymbol{A}} \\ y_{\boldsymbol{B}} \end{bmatrix}$$

5. Use Monte Carlo integration to approximate the first-order Sobol's indices:

$$S_i = \frac{\text{var}\left[\mathbb{E}(y|q_i)\right]}{\text{var}(y)} \approx \frac{\frac{1}{M}\left[y_{\boldsymbol{A}}^{\top} y_{\boldsymbol{C_B^i}} - y_{\boldsymbol{A}}^{\top} y_{\boldsymbol{B}}\right]}{\frac{1}{2M} y_{\boldsymbol{D}}^{\top} y_{\boldsymbol{D}} - \left[\mathbb{E}(y_{\boldsymbol{D}})\right]^2} \tag{30}$$

and total-effects Sobol's indices:

$$S_{Ti} = \frac{\mathbb{E}\left[\text{var}(y|q_{\sim i})\right]}{\text{var}(y)} \approx \frac{\frac{1}{2M}\left[y_{\boldsymbol{A}}^{\top} y_{\boldsymbol{A}} - 2 y_{\boldsymbol{A}}^{\top} y_{\boldsymbol{C_A^i}} + y_{\boldsymbol{C_A^i}}^{\top} y_{\boldsymbol{C_A^i}}\right]}{\frac{1}{2M} y_{\boldsymbol{D}}^{\top} y_{\boldsymbol{D}} - \left[\mathbb{E}(y_{\boldsymbol{D}})\right]^2} \tag{31}$$

where $\mathbb{E}(y_{\boldsymbol{D}}) \approx \dfrac{1}{2M} \displaystyle\sum_{j=1}^{2M} y_{\boldsymbol{D}}^{j}$.

Finally, since the total-effects Sobol's indices consider both first-order effect of q_i and high-order interaction effects involving q_i, we only discuss the results for the total-effects indices. We plot the value of the total-effects indices in Figure 12. It is worth to mention that there are cases where the total-effects indices are negative. However, in these cases, the order of magnitudes are between -16 and -15. Therefore, we consider them as discrepancies due to numerical approximations and plotted their absolute values instead.

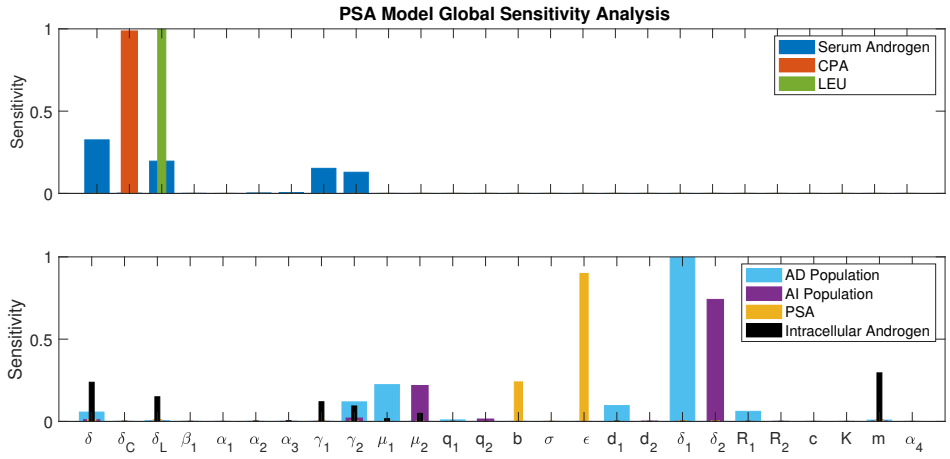

Figure 12: **(Top)** Total-effects Sobol's indices for serum androgen (blue), LEU mass (orange), and CPA mass (green) with respect to each parameter of the full model. **(Bottom)** Total-effects Sobol's indices for androgen-dependent population (blue), androgen-independent population (magenta), intracellular androgen (yellow) and prostate-specific antigen (black) with respect to each parameter of the full New PSA Model. **Note**: δ, δ_1, δ_2, β_1, α_1, α_2, α_3, α_4, γ_1 and γ_2 parameter values are those of the New Androgen Model depicted in Figure 8.

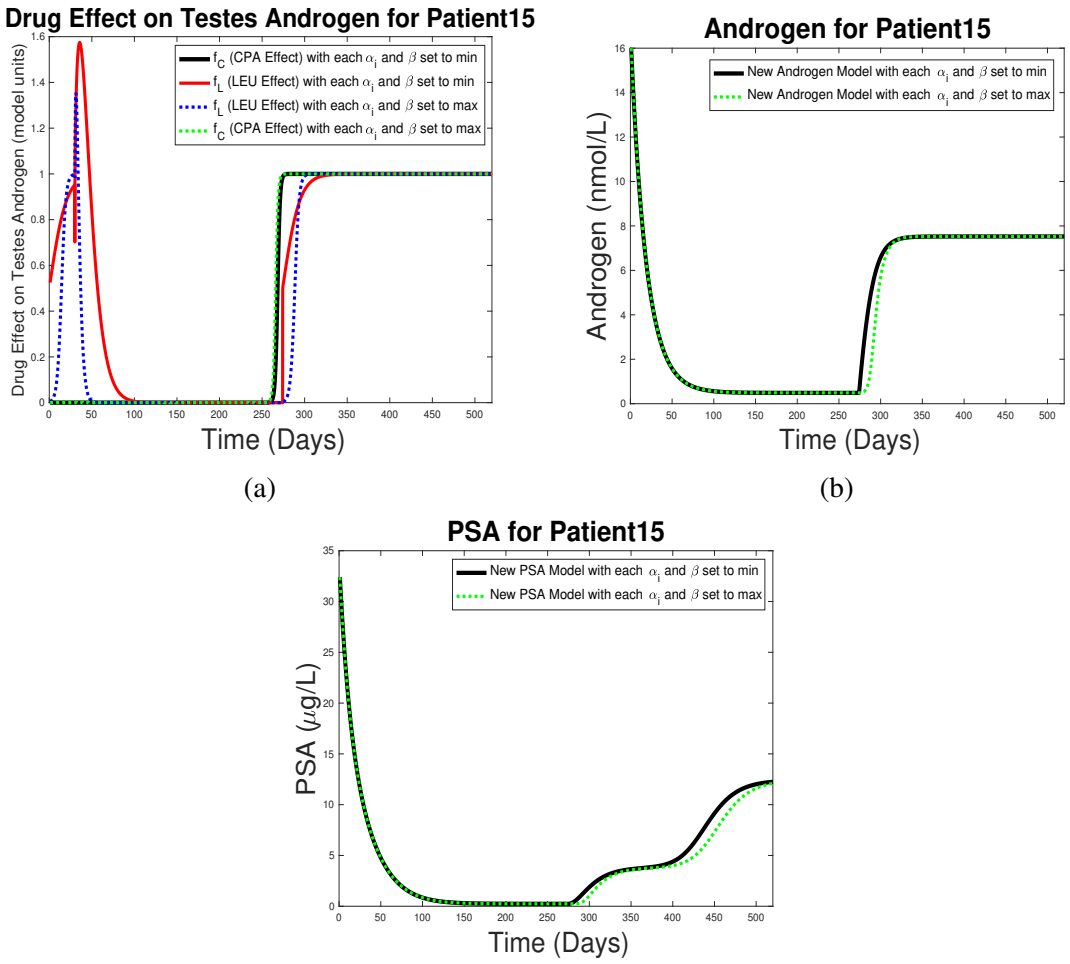

Figure 13: The New Androgen Model and the New PSA Model run over one full cycle (for patient 15, 520 days) with the minimum and maximum values of each respect α_i parameter range and β parameter range. All other parameters remain constant and are pulled from patient 15's fitting.

5.4 Additional Figures

5.4.1 Additional Figures for Dynamics of the New Androgen Model

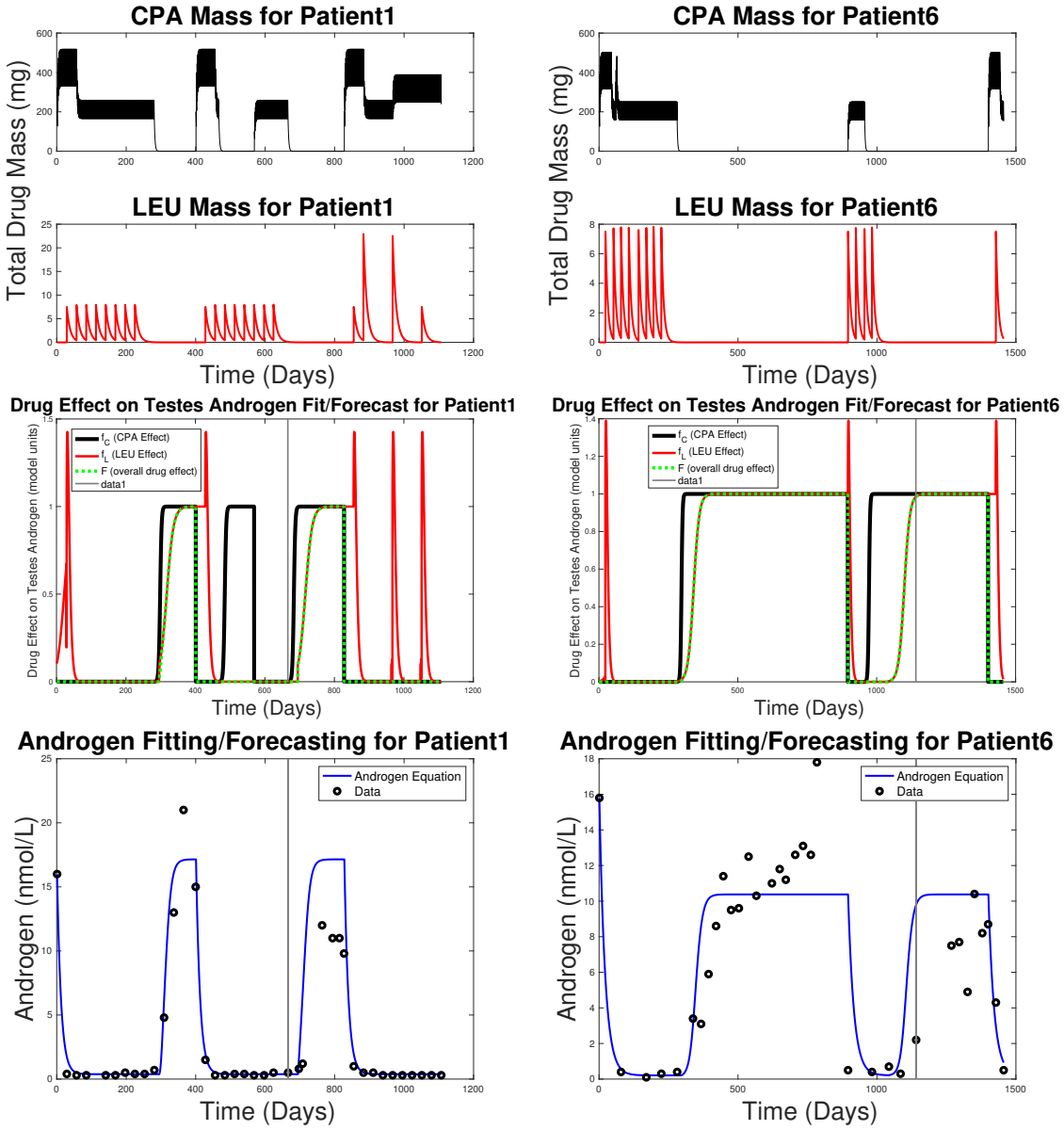

Figure 14: Patient1-specific and patient6-specific New Androgen Model results showing drug amount, drug effects, and androgen fit and forecast. Note the vertical grey line marks the end of the fitting period.

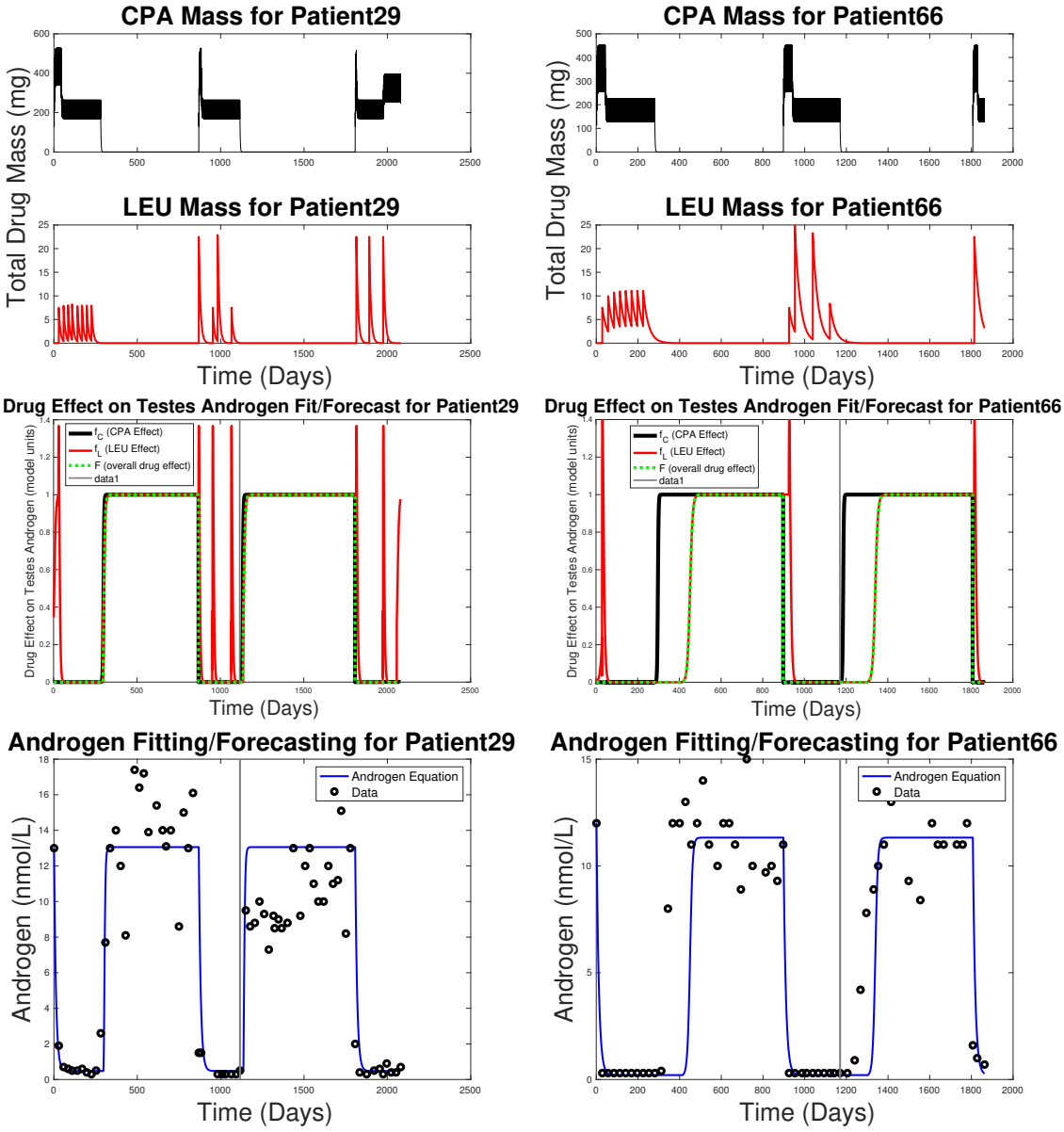

Figure 15: Patient29-specific and patient66-specific New Androgen Model results showing drug amount, drug effects, and androgen fit and forecast. Note the vertical grey line marks the end of the fitting period.

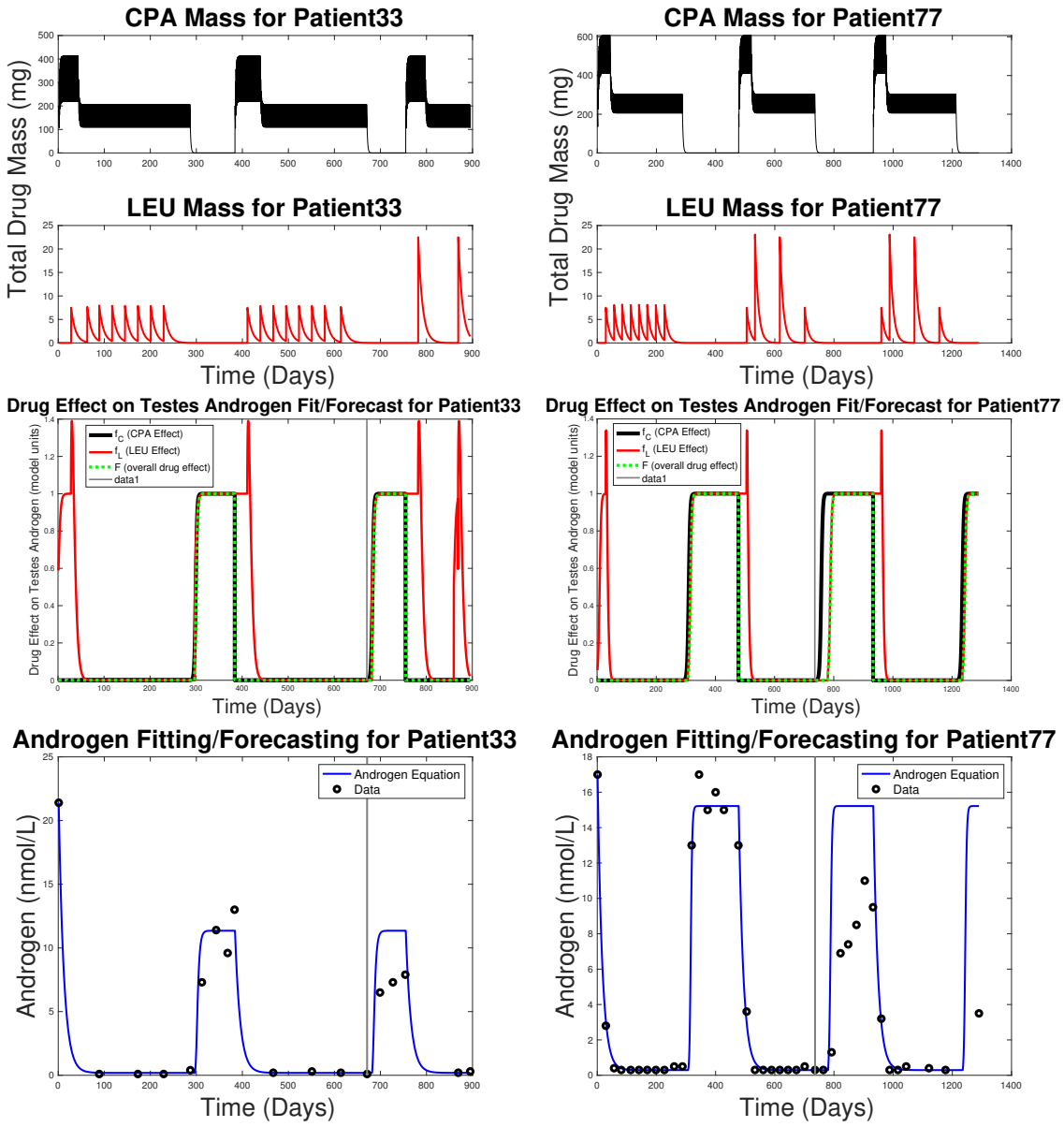

Figure 16: Patient33-specific and patient77-specific New Androgen Model results showing drug amount, drug effects, and androgen fit and forecast. Note the vertical grey line marks the end of the fitting period.

5.4.2 Additional Figures for Androgen Comparison

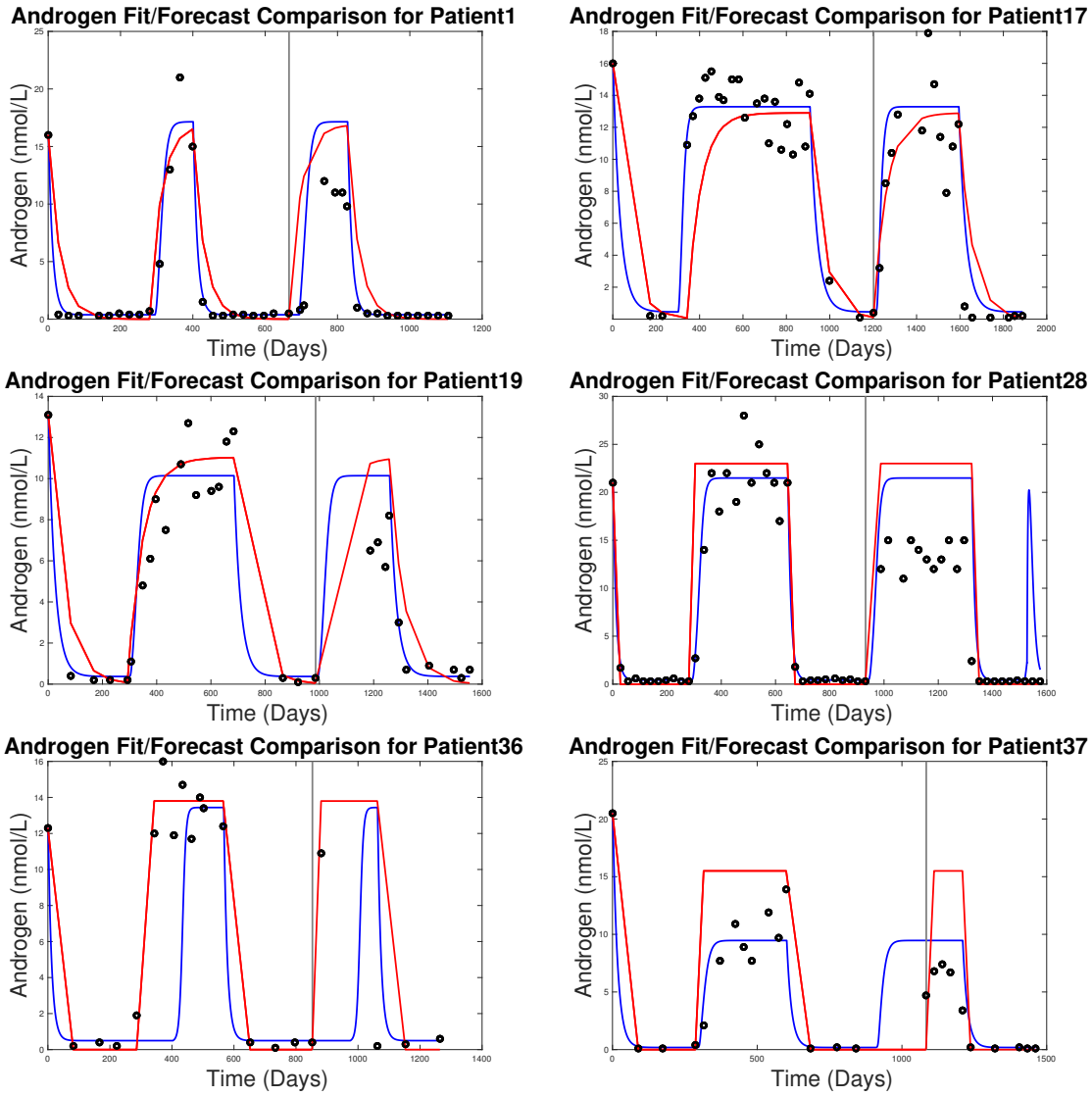

Figure 17: Androgen fitting and forecasting results for the Improved BK model (**red curves**) and New PSA Model (**blue curves**). The fitting and forecasting periods are separated by the vertical line at day 665 for patient 1, day 1201 for patient 17, day 985 for patient 19, day 931 for patient 28, day 852 for patient 36, and day 1083 for patient 37. Fitting and forecasting results are shown for data from patients 1, 17, 19, 28, 36, and 37 (**black circles**). For all models, we fit 1.5 cycles, then forecast the next cycle. For patient 28 the spike at the end occurs in the New Androgen Model due to large gaps in the injecting of LEU. This is a prime example of the need for a mechanisms for a long term effects the drugs have on overall androgen production.

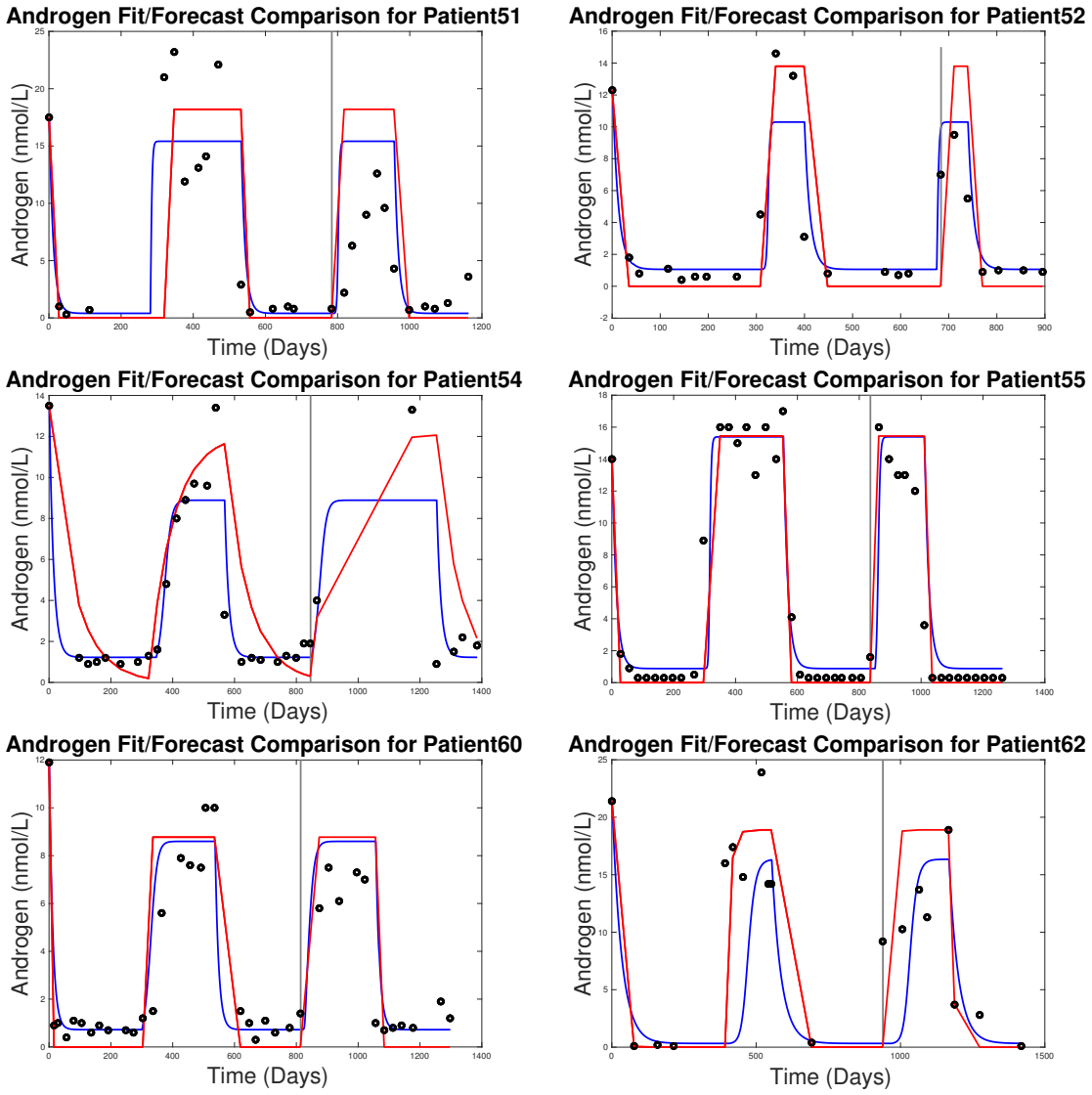

Figure 18: Androgen fitting and forecasting results for the Improved BK model (**red curves**) and New PSA model (**blue curves**). The fitting and forecasting periods are separated by the vertical line at day 783 for patient 51, day 683 for patient 52, day 845 for patient 54, day 835 for patient 55, day 813 for patient 60, and day 938 for patient 62. Fitting and forecasting results are shown for data from patients 51, 52, 54, 55, 60, and 62 (**black circles**). For all models, we fit 1.5 cycles, then forecast the next cycle.

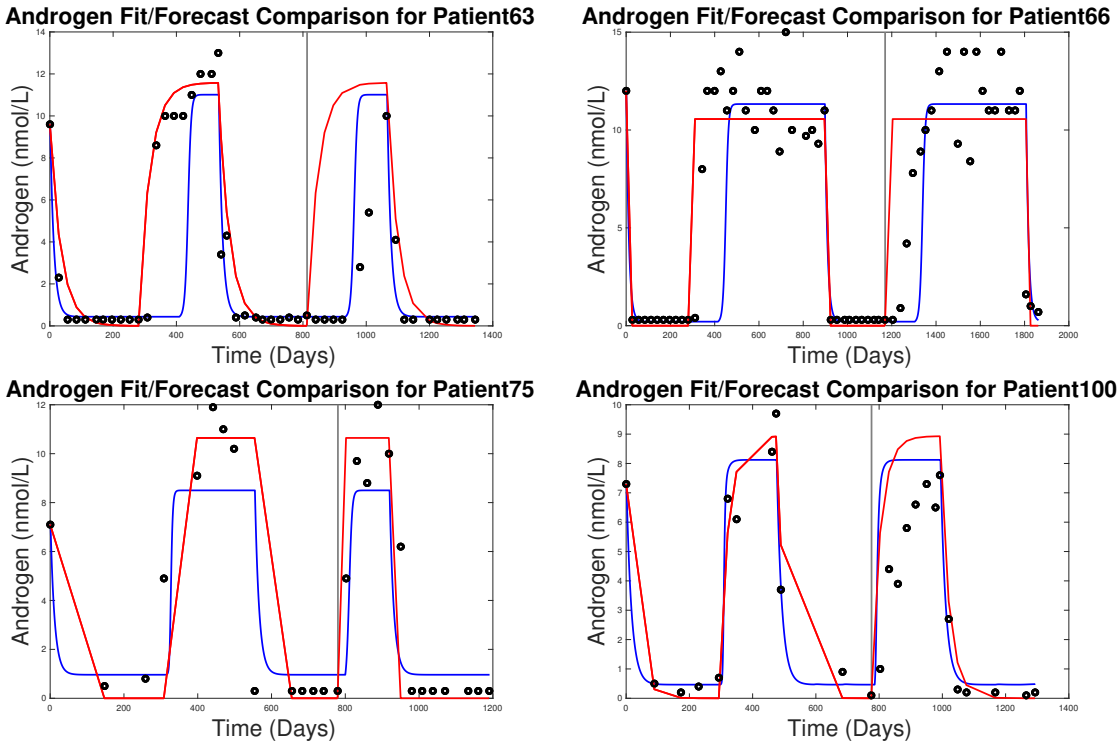

Figure 19: Androgen fitting and forecasting results for the Improved BK model (**red curves**) and New PSA Model (**blue curves**). The fitting and forecasting periods are separated by the vertical line at day 812 for patient 63, day 1169 for patient 66, day 779 for patient 75, and day 775 for patient 100. Fitting and forecasting results are shown for data from patients 63, 66, 75, 100 (**black circles**). For all models, we fit 1.5 cycles, then forecast the next cycle.

5.4.3 Additional Figures for PSA Comparison

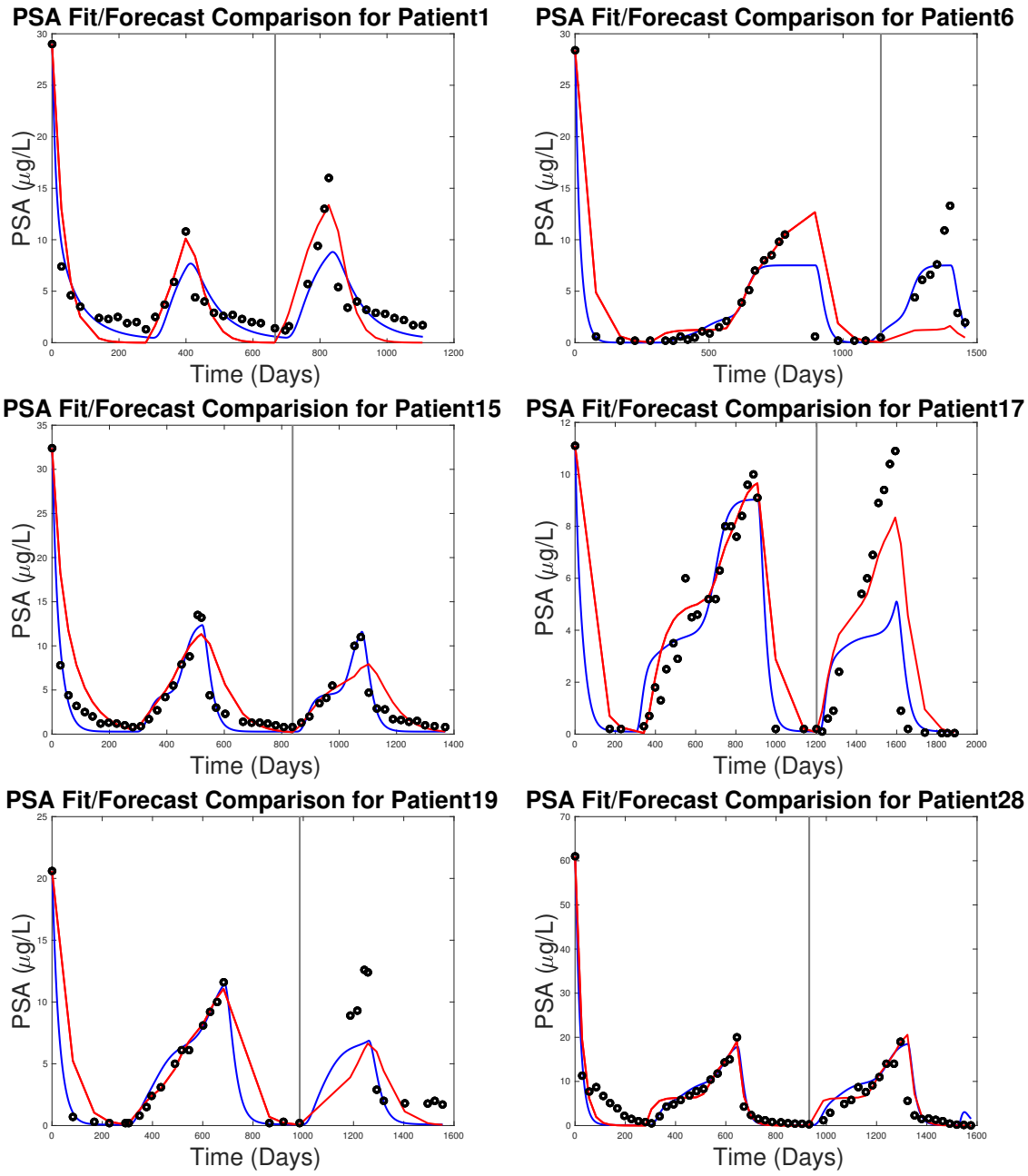

Figure 20: Prostate-specific antigen fitting and forecasting results for the Improved BK model (**red curves**) and New PSA Model (**blue curves**). The fitting and forecasting periods are separated by the vertical line at day 665 for patient 1, day 1140 for patient 6, day 837 for patient 15, day 1201 for patient 17, day 985 for patient 19, and day 931 for patient 28. Fitting and forecasting results are shown for data from patients 1, 6, 15, 17, 19, and 28 (**black circles**). For all models, we fit 1.5 cycles, then forecast the next cycle.

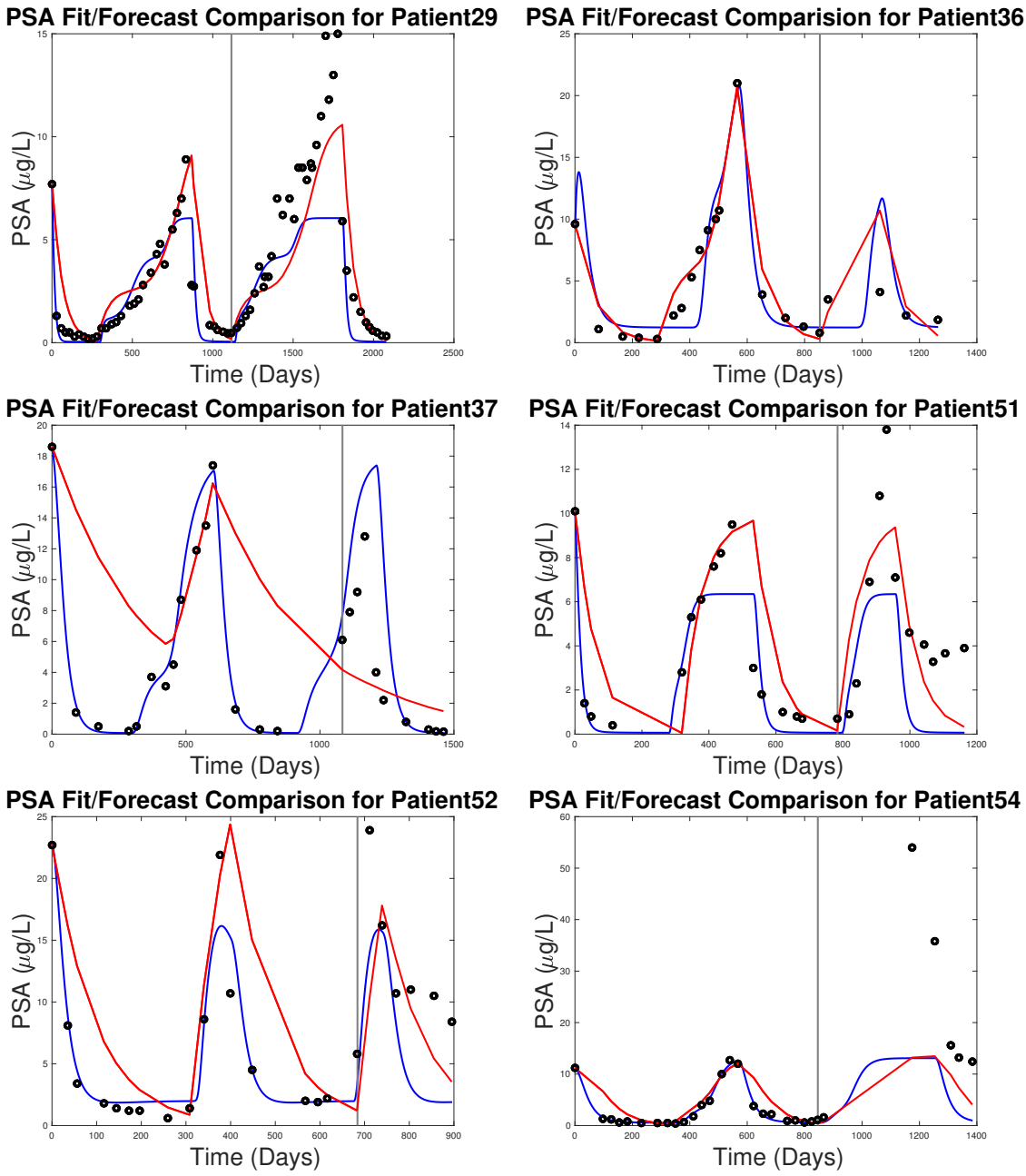

Figure 21: Prostate-specific antigen fitting and forecasting results for the Improved BK model (**red curves**) and New PSA Model (**blue curves**). The fitting and forecasting periods are separated by the vertical line at day 1115 for patient 29, day 852 for patient 36, day 1083 for patient 37, day 783 for patient 51, day 683 for patient 52, and day 845 for patient 54. Fitting and forecasting results are shown for data from patients 29, 36, 37, 51, 52 and 54 (**black circles**). For all models, we fit 1.5 cycles, then forecast the next cycle.

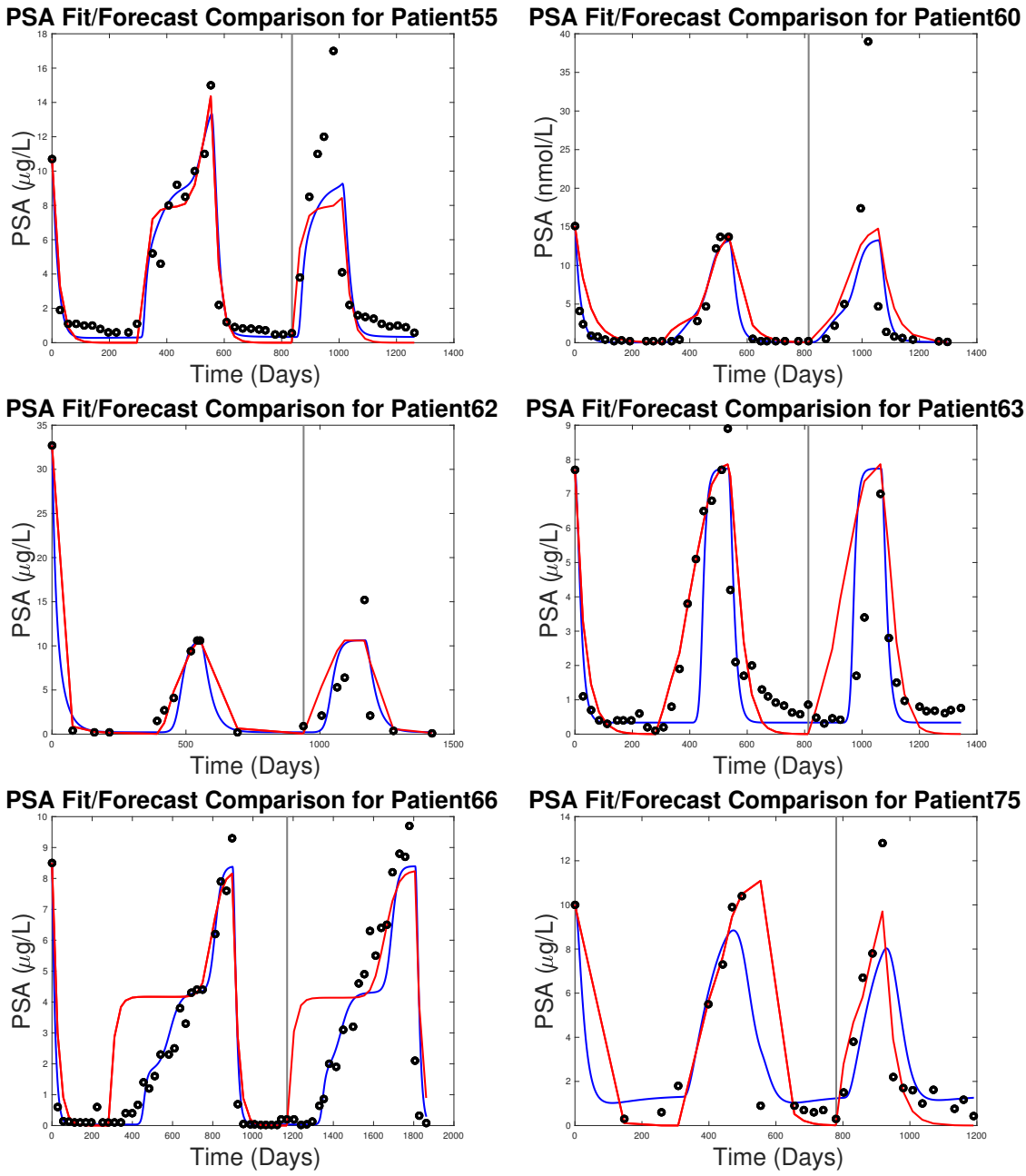

Figure 22: Prostate-specific antigen fitting and forecasting results for the Improved BK model (**red curves**) and New PSA Model (**blue curves**). The fitting and forecasting periods are separated by the vertical line at day 835 for patient 55, day 813 for patient 60, and day 938 for patient 62, day 812 for patient 63, day 1169 for patient 66, and day 779 for patient 75. Fitting and forecasting results are shown for data from patients 55, 60, 62, 63, 66, and 75 (**black circles**). For all models, we fit 1.5 cycles, then forecast the next cycle.

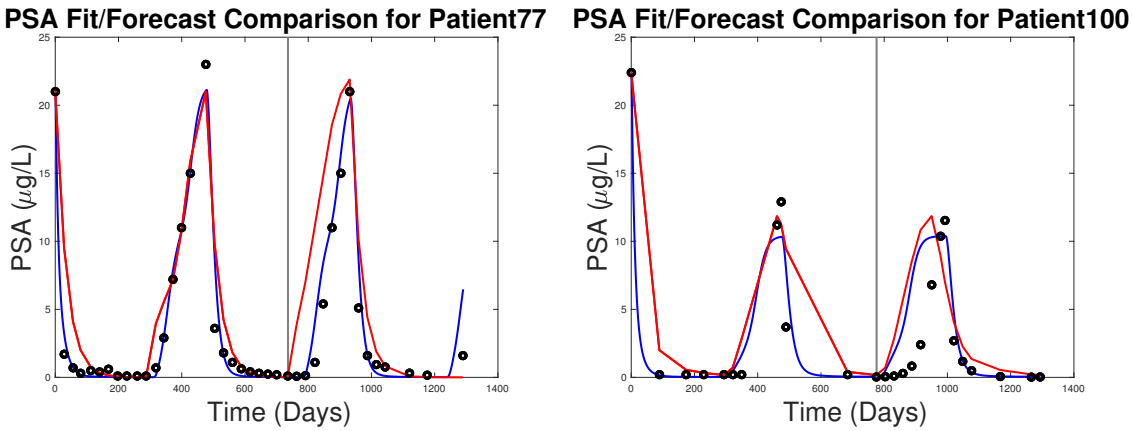

Figure 23: Prostate-specific antigen fitting and forecasting results for the Improved BK model (**red curves**) and New PSA Model (**blue curves**). The fitting and forecasting periods are separated by the vertical line at day 735 for patient 77 and day 775 for patient 100. Fitting and forecasting results are shown for data from patients 77 and 100 (**black circles**). For all models, we fit 1.5 cycles, then forecast the next cycle.

Matlab code used for fitting/forecasting can be provided upon request.